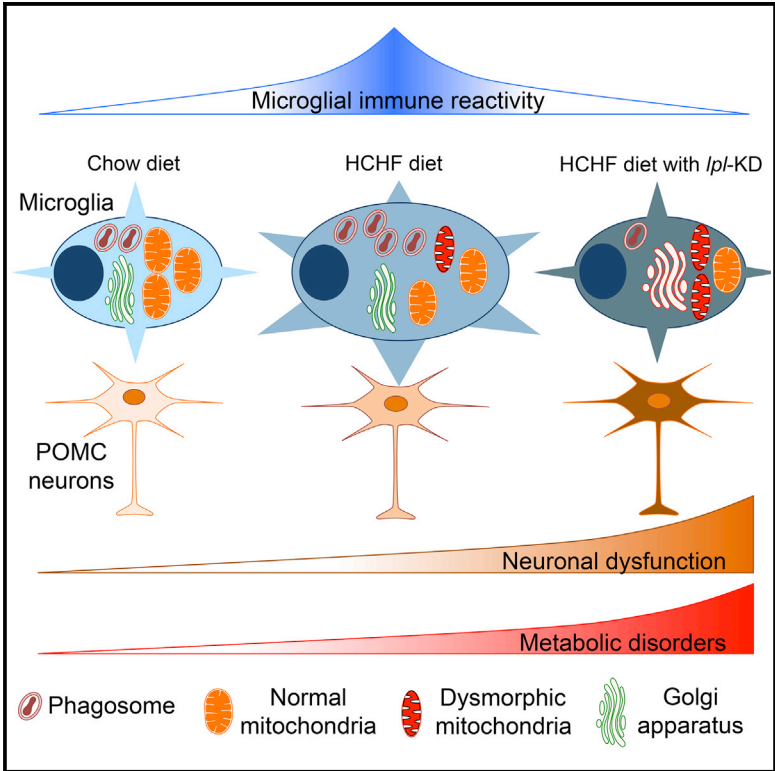


Lipoprotein Lipase Maintains Microglial Innate Immunity in Obesity

Graphical Abstract



Authors

Yuanqing Gao, Andrés Vidal-Itriago, Martin J. Kalsbeek, ..., Robert H. Eckel, Susanna M. Hofmann, Chun-Xia Yi

Correspondence

c.yi@amc.uva.nl

In Brief

Microglia are brain macrophages responsible for immune defense. LPL is a key enzyme gating lipid uptake by microglia. Gao et al. show that loss of *Lpl* in microglia results in downregulation of immune reactivity. Mice with knockdown of the *Lpl* gene in microglia are more vulnerable to diet-induced metabolic syndrome.

Highlights

- High-carbohydrate high-fat diet stimulates microglial *Lpl* gene expression
- Mitochondrial fuel utilization switches to glutamine in microglia lacking LPL
- Microglial immune reactivity is impaired in microglia lacking LPL
- POMC neuronal loss is accelerated when microglia lack LPL



Lipoprotein Lipase Maintains Microglial Innate Immunity in Obesity

Yuanqing Gao,¹ Andrés Vidal-Itriago,¹ Martin J. Kalsbeek,¹ Clarita Layritz,² Cristina García-Cáceres,² Robby Zachariah Tom,³ Thomas O. Eichmann,⁴ Frédéric M. Vaz,⁵ Riekelt H. Houtkooper,⁵ Nicole van der Wel,⁶ Arthur J. Verhoeven,⁷ Jie Yan,⁸ Andries Kalsbeek,^{1,9} Robert H. Eckel,¹⁰ Susanna M. Hofmann,³ and Chun-Xia Yi^{1,11,*}

¹Department of Endocrinology and Metabolism, Academic Medical Center, University of Amsterdam, the Netherlands

²Helmholtz Diabetes Center & German Center for Diabetes Research, Helmholtz Zentrum München & Division of Metabolic Diseases, Technische Universität München, Munich, Germany

³Institute for Diabetes and Regeneration Research & Helmholtz Diabetes Center, Helmholtz Zentrum München, Medizinische Klinik und Poliklinik IV, Klinikum der LMU, Munich, Germany

⁴Institute of Molecular Biosciences, University of Graz, Austria

⁵Laboratory Genetic Metabolic Diseases, Academic Medical Center, University of Amsterdam, the Netherlands

⁶Cellular Imaging Core Facility, Academic Medical Center, University of Amsterdam, the Netherlands

⁷Department of Medical Biochemistry, Academic Medical Centre, University of Amsterdam, the Netherlands

⁸Department of Forensic Science, School of Basic Medical Science, Central South University, Changsha, Hunan, China

⁹Hypothalamic Integration Mechanisms, Netherlands Institute for Neuroscience, Amsterdam, the Netherlands

¹⁰Division of Endocrinology, Metabolism and Diabetes, University of Colorado School of Medicine, Aurora, CO, USA

¹¹Lead Contact

*Correspondence: c.yi@amc.uva.nl

<http://dx.doi.org/10.1016/j.celrep.2017.09.008>

SUMMARY

Consumption of a hypercaloric diet upregulates microglial innate immune reactivity along with a higher expression of lipoprotein lipase (*Lpl*) within the reactive microglia in the mouse brain. Here, we show that knockdown of the *Lpl* gene specifically in microglia resulted in deficient microglial uptake of lipid, mitochondrial fuel utilization shifting to glutamine, and significantly decreased immune reactivity. Mice with knockdown of the *Lpl* gene in microglia gained more body weight than control mice on a high-carbohydrate high-fat (HCHF) diet. In these mice, microglial reactivity was significantly decreased in the mediobasal hypothalamus, accompanied by downregulation of phagocytic capacity and increased mitochondrial dysmorphologies. Furthermore, HCHF-diet-induced POMC neuronal loss was accelerated. These results show that LPL-governed microglial immunometabolism is essential to maintain microglial function upon exposure to an HCHF diet. In a hypercaloric environment, lack of such an adaptive immunometabolic response has detrimental effects on CNS regulation of energy metabolism.

INTRODUCTION

Microglia are brain macrophages responsible for innate immune reactivity, which is essential for maintaining a local microenvironment optimal for neuronal survival and functioning (Kettenmann et al., 2011; Li et al., 2012; Prinz and Priller, 2014). In high-carbohydrate high-fat (HCHF)-diet-induced obese mice,

microglial reactivity in the hypothalamus increases (Gao et al., 2014; Thaler et al., 2012). Intracellular metabolism is closely related with the function of immune cells (O'Neill et al., 2016). Activated immune cells such as macrophages and T cells have high metabolic demands (Newsholme et al., 1986; Oren et al., 1963) and thus require a higher fuel influx. One of the key enzymes involved in cellular fuel uptake is lipoprotein lipase (LPL), the enzyme that delivers lipids by catalyzing triglyceride (TG)-rich lipoproteins (Wang and Eckel, 2009). On a high-fat atherogenic diet, LPL in mouse macrophages is important for promoting foam cell formation through the degradation and internalization of lipoproteins (Babaev et al., 1999). Among the different types of brain cells, microglia show the highest level of *Lpl* mRNA expression (Zhang et al., 2014; Zhang et al., 2016). When we compared isolated hypothalamic microglia from standard chow-diet-fed lean mice and HCHF-diet-induced obesity (DIO) mice, we detected a significant increase in *Lpl* gene expression in DIO mice, indicating that LPL might be involved in the activation of hypothalamic microglia in animals on an HCHF diet. We therefore generated ex vivo and in vivo models with microglia-specific knockdown of the *Lpl* gene and studied microglial immunometabolism and hypothalamic neural responses to hypercaloric challenges.

RESULTS

Lpl Gene Expression Is Highest in Hypothalamic Microglia

In primary cultured hypothalamic neurons, astrocytes, and microglia, we observed the highest *Lpl* mRNA level in microglia (Figure 1A). In isolated hypothalamic microglia from mice that had been on an HCHF diet for 1 day, 3 days, 7 days, 28 days, or 10 weeks, microglial *Lpl* gene expression increased after 3 days on the HCHF diet compared with mice on a chow diet, except for a transient decline on day 7 (Figure 1B). These data

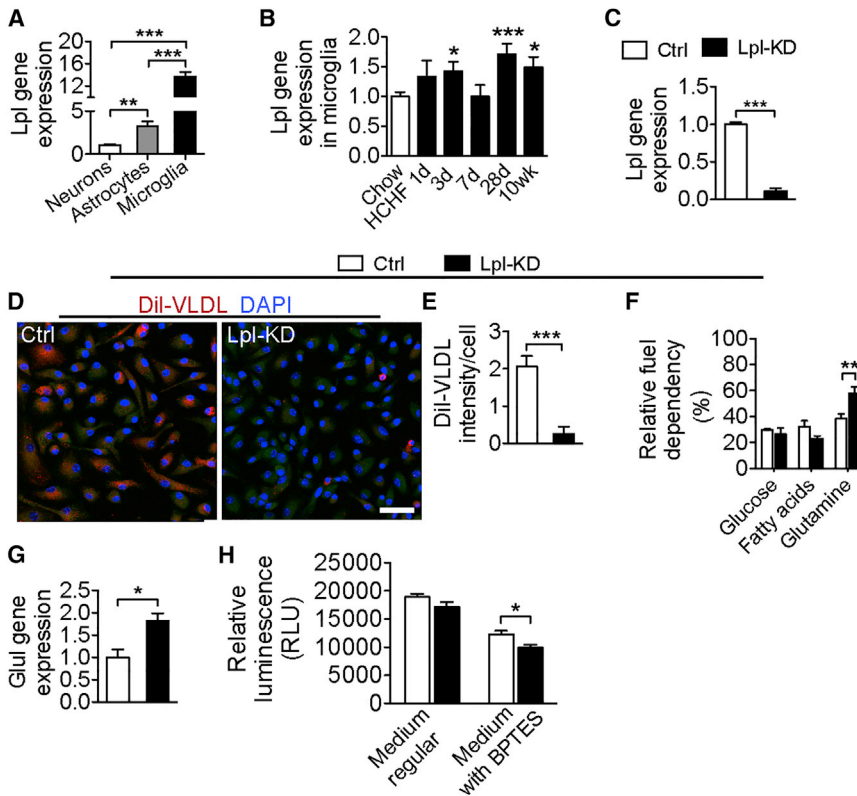


Figure 1. LPL in Microglia Governs Microglial Immunometabolism

(A) *Lpl* mRNA levels in hypothalamic primary neurons (n = 5), astrocytes (n = 4), and microglia (n = 3). (B) The *Lpl* mRNA level is higher in hypothalamic microglia isolated from mice on an HCHF diet for 3 days, 28 days, and 10 weeks (n = 4–11) than from chow-diet-fed mice (n = 7). (C) The *Lpl* mRNA level is significantly down-regulated in *Lpl*-KD microglia in primary cultures with 5 days of 4-hydroxytamoxifen treatment; n = 7 per group. (D) Dil-VLDL uptake in primary microglia. (E) Dil-VLDL uptake is significantly blocked in primary *Lpl*-KD microglia, n = 6 per group. (F) Relative fuel dependency in Ctrl microglia (n = 6–11) and *Lpl*-KD microglia (n = 7–11). (G) The glutamine synthetase (*Glul*) mRNA level is significantly increased in isolated microglia from microglia-*Lpl*-KD mouse brains; n = 4 per group. (H) The *Lpl*-KD microglia survival rate (indicated by relative luminescence) is decreased by the glutaminase inhibitor BPTES; n = 7 per group. Data are presented as mean ± SEM. *p < 0.05, **p < 0.01, ***p < 0.001. Unpaired t test was performed in all experiments. Scale bar, 20 μm.

suggest that microglial LPL might be involved in the hypothalamic mechanisms that regulates energy metabolism.

Lack of Microglial LPL Disrupts Intracellular Lipid Metabolism

Next, we generated ex vivo primary cultured microglia with a deletion of the *Lpl* gene. Mice carrying loxP-flanked *Lpl* alleles (*Lpl*^{fl/fl}, C57BL/6 background) were crossed with mice carrying tamoxifen-inducible CRE recombinase driven by the *Cx3cr1* promoter (*Cx3cr1*^{CreERT2}, C57BL/6 background). Primary microglia from *Lpl*^{fl/fl}-*Cx3cr1*^{CreERT2} mice were used to generate *Lpl* knockdown microglia (*Lpl*-KD, mixed gender). Primary microglia from *Cx3cr1*^{CreERT2} mice were used as a control (Ctrl). All primary microglia were treated with 4-hydroxytamoxifen to induce deletion of the *Lpl* gene. Successful knockdown (KD) was confirmed by the decrease of *Lpl* mRNA in *Lpl*-KD microglia compared with the Ctrl (Figure 1C).

To test the uptake capacity of TG-rich lipoproteins, *Lpl*-KD microglia and Ctrl cells were incubated with very-low-density lipoprotein (VLDL) particles labeled with the fluorescent dye Dil (VLDL-Dil), which can be taken up by hypothalamic microglia (Valdearcos et al., 2014). Abundant Dil signals were detected in Ctrl microglia but not in *Lpl*-KD microglia (Figures 1D and 1E), indicating a significant downregulation of lipid uptake in *Lpl*-KD microglia.

Subsequently, we found a significant decrease in major phospholipid species, including glycerophosphoethanolamines, glycerophosphocholines, and glycerophosphoinositols, in *Lpl*-

KD microglia (Figures S1A–S1C), suggesting a disrupted intracellular lipid metabolism in microglia that lack LPL.

Microglia Lacking LPL Shift Mitochondrial Fuel Utilization to Glutamine

To investigate whether the changes in intracellular lipid metabolism in *Lpl*-KD microglia affect the fuel utilization by these cells, we examined the oxidative substrate preference of microglia by a mitochondrial fuel flex assay. In this assay, inhibitors were added in a different order and in pre-designed combinations to calculate dependency on glucose, fatty acid, and glutamine oxidation from the changes in oxygen consumption rate (OCR). Glucose and total fatty acid dependencies were not significantly changed in *Lpl*-KD microglia (Figure 1F; Figures S1D and S1E), although fatty acid dependency showed a trend toward decrease in *Lpl*-KD microglia. Interestingly, glutamine dependency was significantly increased in *Lpl*-KD microglia (Figure 1F; Figure S1F). We also found that glutamine synthetase gene expression was elevated in microglia isolated from microglial *Lpl*-KD adult mouse brain compared with those from Ctrl mouse brains (Figure 1G). Glutamine synthetase is an enzyme that catalyzes the formation of glutamate from glutamate. Consistently, by visualizing *glutamate* aspartate transporter (GLAST)-EGFP in GLAST^{CreERT2}-tdTomato-EGFP mice (García-Cáceres et al., 2016), we found GLAST gene expression in microglia (Figures S1G–S1J), confirming that glutamine can be synthesized from intracellular glutamate. However, we also found that the total cellular glutamine and glutamate levels did

not change in *Lpl*-KD microglia (Figures S1K and S1L), suggesting a higher turnover of the glutamine-glutamate cycles in these cells. Thus, *Lpl*-KD microglia are able to shift their fuel utilization to glutamine to compensate for the reduced utilization of fatty acids. We then found that inhibition of glutaminase by *N,N'*-[thiobis(2,1-ethanediy)-1,3,4-thiadiazole-5,2-diy]] bisbenzeneacetamide (BPTES) resulted in a significant decrease in primary microglial survival rates in *Lpl*-KD microglia (Figure 1H), implying an essential role of glutamine-derived glutamate for cell survival under *Lpl*-KD conditions.

To further confirm these results, we used a fluorescent glucose analog, 2-deoxy-2-[(7-nitro-2,1,3-benzoxadiazol-4-yl)amino]-D-glucose (2-NBDG), to evaluate microglial glucose uptake. With 10 min of 2-NBDG incubation in primary microglia at a concentration of 10 μ M, we found no differences between *Lpl*-KD microglia and Ctrl microglia (Figures S1M and S1N). Also, we detected no differences in gene expression of *Glut1* and *Glut5* between microglia isolated from microglial *Lpl*-KD and Ctrl mouse brains (Figure S1O). Together with our OCR measurements, these findings indicate that cellular glucose metabolism was not significantly affected in microglia lacking LPL.

Microglia Lacking LPL Show Attenuated Immune Response and Phagocytic Capacity

To evaluate microglial immune reactivity in response to immune challenges, we treated microglia with lipopolysaccharide (LPS). We found that tumor necrosis factor alpha (TNF- α) gene expression was significantly lower in *Lpl*-KD microglia (Figure S2A). Because high-fat-diet-derived fatty acids have been found to be one of the major stimuli for microglial activation (Valdearcos et al., 2014), we measured the microglial immune response to palmitic acid (PA). *Tnf- α* gene expression in *Lpl*-KD microglia was profoundly decreased compared with Ctrl microglia (Figure S2A). Because TNF- α produced by microglia is a critical autocrine mediator in microglial activation (Kuno et al., 2005), we checked phospho-nuclear factor κ B (NF- κ B) after TNF- α stimulation and found a significant decrease in phospho-NF- κ B in *Lpl*-KD microglia (Figures S2B and S2C). These data indicate an overall attenuated inflammatory response upon pro-inflammatory stimuli in microglia lacking LPL.

To examine whether the attenuated immune response in microglia is associated with changes in their phagocytic capacity, we measured the uptake of microspheres in primary microglia. In *Lpl*-KD microglia, the uptake of microspheres was significantly reduced compared with that of Ctrl microglia (Figures S2D and S2E), indicating that lacking LPL impairs microglial phagocytic capacity.

Generation of an Animal Model with Postnatal Microglia-Specific Deletion of *Lpl*

To further understand the function of microglial pathophysiology in vivo, we generated a mouse model with specific deletion of the *Lpl* gene from brain microglia at the adult stage. The use of the *Cx3cr1*-Cre^{ERT2} mouse model for brain microglia-specific gene modification has been characterized in detail in previous studies (Goldmann et al., 2013; Yona et al., 2013). Briefly, *Lpl*^{fl/fl} mice were crossed with *Cx3cr1*^{CreERT2} mice as described above.

Male *Lpl*^{fl/fl}-*Cx3cr1*^{CreERT2} mice were used for these experiments. After giving tamoxifen to *Lpl*^{fl/fl}-*Cx3cr1*^{CreERT2} mice at 6 weeks of age, the *Lpl* gene was deleted from microglia and blood mononuclear myeloid cells (Figure S2F). Upon tamoxifen withdrawal, within 2–3 weeks, *Lpl* gene-deleted mononuclear myeloid cells in the periphery were replenished with newly generated wild-type mononuclear myeloid cells from the bone marrow, whereas microglia in the brain retained *Lpl* gene KD (microglia-*Lpl*-KD).

To validate *Lpl* gene deletion, total DNA was isolated from brain and blood mononuclear myeloid cells of microglia-*Lpl*-KD and Ctrl mice 4 weeks and/or 10 weeks after tamoxifen injection and used for PCR analysis. After Cre-induced recombination at the flox site spanning *Lpl* exon 1, a delta band of 409 bp appeared in microglia-*Lpl*-KD mouse brains isolated at week 4 after tamoxifen injection (Figure S2G) but not in blood mononuclear myeloid cells of microglia-*Lpl*-KD mice isolated at week 4 after tamoxifen injection (Figure S2G). At week 10 after tamoxifen injection, we also detected the delta band in hypothalamic tissue of microglia-*Lpl*-KD mice (Figure 2A), thus confirming that *Lpl* gene expression was significantly decreased in these microglia compared with those of Ctrl (Figure 2B). Together, these data demonstrate that tamoxifen-induced Cre recombination occurs in microglia and other populations of long-lived myeloid cells in the CNS, including perivascular macrophages that express *Cx3cr1*.

Mice with Microglia-Specific *Lpl* Deletion on an HCHF Diet Show an Exaggerated Metabolic Phenotype

To evaluate the functional significance of LPL in microglia under physiological and hypercaloric diet conditions, we fed microglia-*Lpl*-KD and Ctrl mice a standard chow or an HCHF diet. Interestingly, the body weight gain, food intake, and body composition of chow-diet-fed microglia-*Lpl*-KD mice were similar to that of Ctrl mice (Figures S2H–S2K). On an HCHF diet, microglia-*Lpl*-KD mice had a similar daily food intake as Ctrl (Figure 2C). Also, no differences in food intake were found in fasting-refed tests on an HCHF diet (data not shown). However, microglia-*Lpl*-KD mice had accelerated body weight gain (Figure 2D), which can be attributed to greater fat mass gain (Figure 2E). Glucose intolerance induced by the HCHF diet was exaggerated in microglia-*Lpl*-KD mice compared with Ctrl (Figure 2F). Although locomotor activity did not differ between Ctrl and microglia-*Lpl*-KD mice on a daily basis (Figure 2G), microglia-*Lpl*-KD mice did have lower heat production during the light phase, indicating less energy expenditure during the resting period (Figure 2H). Because food intake was not different between Ctrl and microglia-*Lpl*-KD mice, reduced heat production might be the major cause of the body weight gain (Tschöp et al., 2011). Furthermore, the respiratory exchange rate (RER) was significantly lower in microglia-*Lpl*-KD mice (Figure 2I), indicating that microglia-*Lpl*-KD mice used more lipids as an energy substrate than Ctrl mice, possibly because of their greater adiposity. These data demonstrate that mice with a microglia-specific *Lpl* deletion were unable to maintain the CNS mechanisms that control systemic glucose and energy metabolism at the proper level when on an HCHF diet.

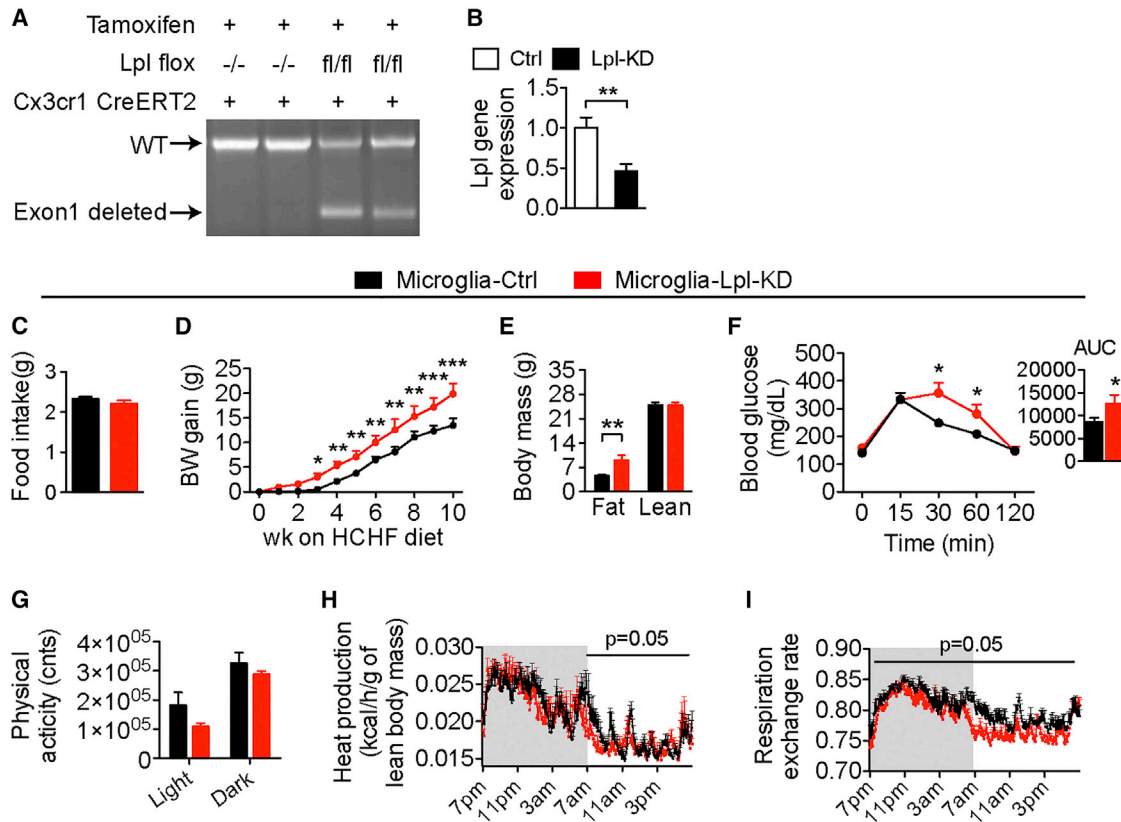


Figure 2. Mice Lacking LPL in Microglia Have Exaggerated Metabolic Disorders on an HCHF Diet

(A) Efficient deletion of the *Lpl* gene is shown by recombined DNA sequence after *Lpl* exon 1 deletion in microglia-*Lpl*-KD mice by PCR in homogenized hypothalamic tissue.

(B) The *Lpl* mRNA level is significantly downregulated in microglia isolated from microglia-*Lpl*-KD mouse brains; n = 6 per group.

(C) Food intake on an HCHF diet does not change in microglia-*Lpl*-KD mice; n = 6–8 per group.

(D) The body weight gain of microglia-*Lpl*-KD mice (n = 11) is significantly greater than that of Ctrl mice (n = 18).

(E) Fat mass is significantly higher in microglia-*Lpl*-KD mice; n = 5–6 per group.

(F) Blood glucose level at 30 and 60 min during a glucose tolerance test are significantly higher in microglia-*Lpl*-KD mice; n = 5–8 per group.

(G) Physical activity does not differ between control and microglia-*Lpl*-KD mice; n = 4 per group.

(H) There is significant lower heat production in microglia-*Lpl*-KD mice during the light phase, n = 4 per group.

(I) There is an effect of genotype on the respiration exchange rate in microglia-*Lpl*-KD mice during the light-dark cycle; n = 4 per group.

Data are presented as mean ± SEM. *p < 0.05, **p < 0.01, ***p < 0.001. Unpaired t test was performed in (D) and (E) and in the area under the curve (AUC) in (F). Two-way ANOVA was performed in (F). Repeated measures ANOVA was performed in (H) and (I).

Microglial Immune Reactivity to an HCHF Diet Is Decreased in the Mediobasal Hypothalamus of Mice with a Microglia-Specific *Lpl* Deletion

To investigate the mechanism behind the metabolic disorders of microglia-*Lpl*-KD mice on an HCHF diet, we examined microglia reactivity in the medial basal hypothalamus (MBH)—the key CNS region regulating systemic energy metabolism. Microglia reactivity was evaluated by iba1 immunoreactivity (iba1-ir). On a standard chow diet, the iba1-ir microglia number, soma size, primary projections, and branching in microglia-*Lpl*-KD mice did not differ from Ctrl mice (Figures S3A–S3E). On an HCHF diet, the iba1-ir microglia number in Ctrl mice was significantly increased compared with that of mice on a chow diet, as we reported previously (Gao et al., 2014). However, iba1-ir microglia number, soma size, primary projections, and branching were significantly decreased in

microglia-*Lpl*-KD mice on an HCHF diet compared with Ctrl mice on an HCHF diet (Figures 3A–3E).

Because phagocytosis represents a key process in microglial immunity (Heneka et al., 2015), we subsequently evaluated the phagocytic capacity of microglia. CD68 was used as the in vivo phagocytic indicator. On a chow diet, we found no differences between microglia-*Lpl*-KD and Ctrl mice (Figures S3F and S3G). However, on an HCHF diet, significantly fewer CD68 ir-positive particles were found in microglia from microglia-*Lpl*-KD mice in comparison with Ctrl mice (Figures 3F and 3G). Consistent with this, we also found CD68 gene expression to be decreased in the MBH of microglia-*Lpl*-KD mice on an HCHF diet (Figure 3H). Thus, deletion of the *Lpl* gene in microglia significantly attenuated microglial reactivity and phagocytic capacity in the MBH when the mice were exposed to an HCHF diet.

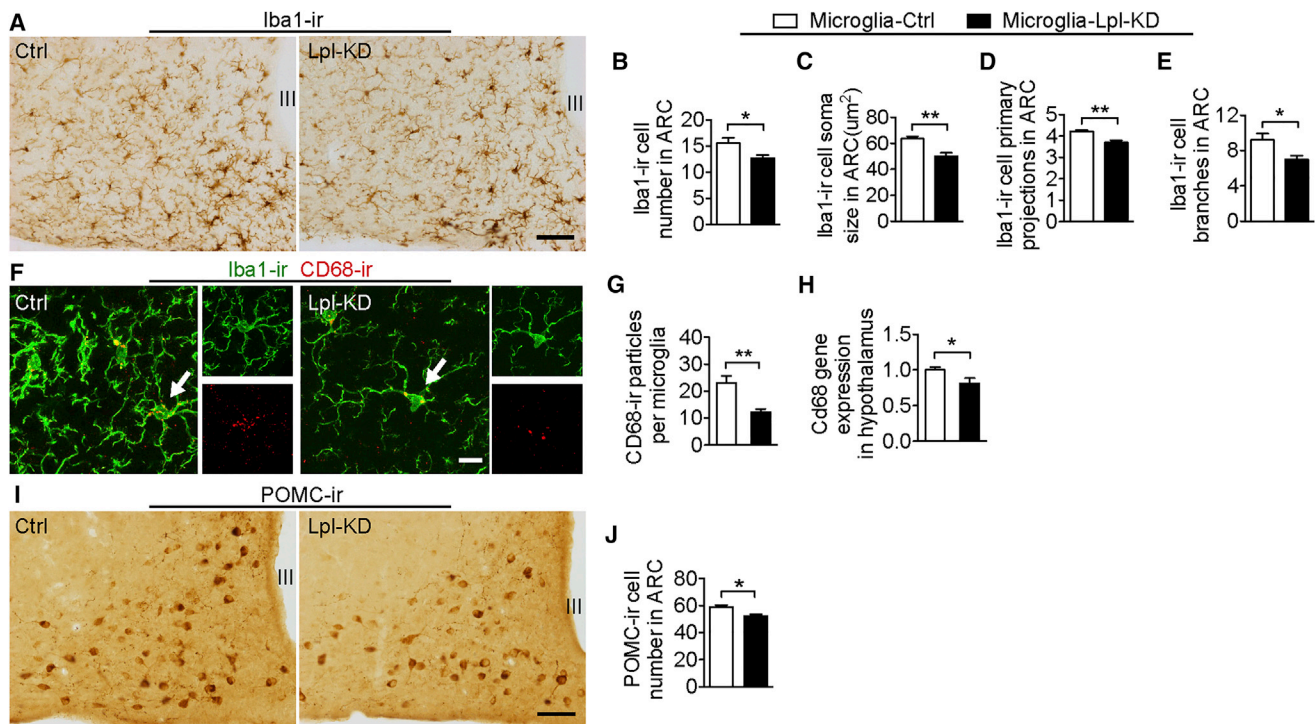


Figure 3. Reduced Microglial Immune Reactivity and Fewer POMC Neurons in the Mediobasal Hypothalamus of Microglia-*Lpl*-KD Mice on an HCHF Diet

(A) Iba1-ir microglia in MBH.

(B–E) The Iba1-ir microglial cell number (B), soma size (C), primary projection (D), and branches (E) are significantly lower in microglia-*Lpl*-KD mouse MBHs on an HCHF diet; n = 7 per group.

(F and G) CD68-ir particles per microglia are significantly lower in microglia-*Lpl*-KD mouse MBHs on an HCHF diet; n = 3–4 per group.

(H) *Cd68* gene expression in HCHF-diet-fed microglia-*Lpl*-KD mouse MBHs are significantly lower; n = 5–7 per group.

(I) POMC-ir in MBH.

(J) The POMC-ir neuronal number is significantly lower in microglia-*Lpl*-KD mouse MBHs on an HCHF diet; n = 7–13 per group.

III, third ventricle. Data are presented as mean ± SEM. *p < 0.05, **p < 0.01. Unpaired t test was performed in all experiments. Scale bars, 100 μm in (A) and (I) and 10 μm in (F).

Diet-induced microglial activation has also been found to be involved in hippocampal dysfunction in memory (Hao et al., 2016). We found that, in Ctrl mice, 10-weeks of the HCHF diet increased Iba1-ir cell branches, but not cell numbers, compared with the chow diet. This increase was significantly reduced in microglia-*Lpl*-KD mice on an HCHF diet (Figure S3H). Thus, our data confirmed that an HCHF diet could impair hippocampus-dependent memory and that this impairment could be affected by deletion of *Lpl* from microglia.

Mice with a Microglia-Specific *Lpl* Deletion Have Accelerated Decrease of POMC Neurons When on an HCHF Diet

Among others, the MBH contains the orexigenic agouti-related peptide (AgRP)-neuropeptide Y (NPY) neurons and anorexigenic proopiomelanocortin (POMC) neurons. Comparing the POMC and NPY neurons, we observed that reactive microglia were more often adjacent to POMC neurons than to NPY neurons (Figures S3I and S3J), as also observed previously (Yi et al., 2017). We therefore examined POMC neurons in the MBH of our microglia-*Lpl*-KD mice. On a chow diet, the

POMC-ir neuron number did not differ between microglia-*Lpl*-KD and Ctrl mice (Figures S3K and S3L), but with an HCHF diet, we observed significantly fewer POMC-ir neurons in microglia-*Lpl*-KD mice compared with Ctrl mice (Figures 3I and 3J).

Microglia-Specific *Lpl* Deletion Results in Mitochondrial Dysfunction in Both Microglia and Nearby Neurons When on an HCHF Diet

Mitochondria are important cellular organelles involved in innate immune signaling pathways (Nakahira et al., 2011; West et al., 2011). To investigate whether the attenuated immunity in *Lpl*-KD microglia is linked to mitochondrial dysfunction, we analyzed the mitochondrial ultrastructure of microglia in the MBH (Figures 4A and 4B).

In comparison with normal mitochondria (Figure 4C1), dysmorphic mitochondria in MBH microglia were characterized by a lower matrix electron density (Figure 4C2), disrupted crista structure (Figure 4C3), and inclusions (Figure 4C4). On a chow diet, there was a significant increase, from 19% to 40%, of dysmorphic microglial mitochondria in the MBH of

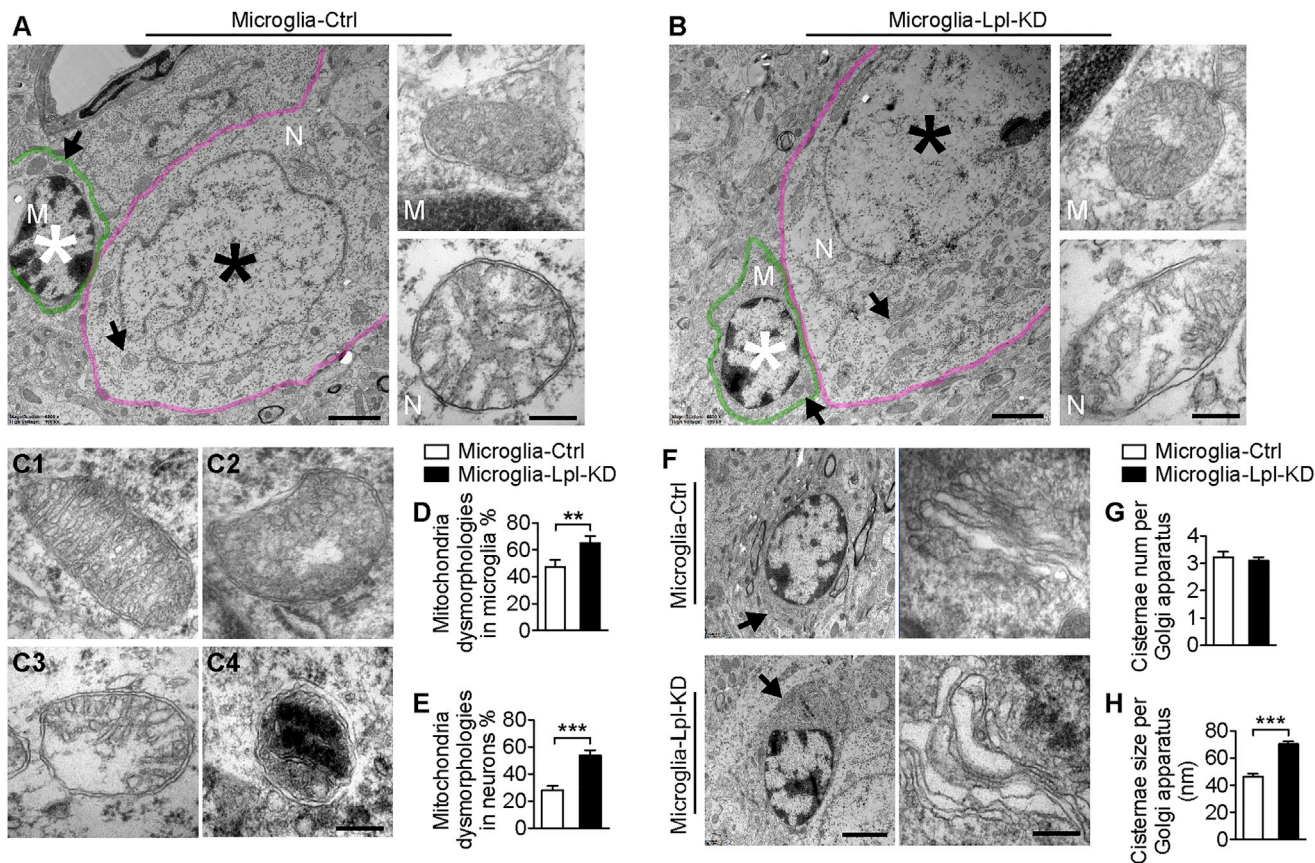


Figure 4. Dysmorphic Mitochondria and Golgi Apparatus in Microglia and Adjacent Neurons in the MBHs of Microglia-*Lpl*-KD Mice

(A and B) Ultrastructure of mitochondria in microglia (M, outlined by a green line) and adjacent neurons (N, outlined by a pink line) in the MBHs of Ctrl (A) and microglia-*Lpl*-KD (B) mice fed an HCHF diet. High magnifications of the mitochondrion in each cell (dark arrows) are shown at the right. *, nucleus of each cell. (C1–C4) Normal mitochondrion (C1) and dysmorphic mitochondrion with less electron density (C2), disrupted crista structure (C3), and inclusions (C4).

(D) The dysmorphic mitochondrion ratio in microglia in the MBH is significantly higher in microglia-*Lpl*-KD mice than in Ctrl mice on an HCHF diet.

(E) The dysmorphic mitochondrion ratio in neurons adjacent to microglia in the MBH is significantly higher in microglia-*Lpl*-KD mice than in Ctrl mice on an HCHF diet.

(F) Golgi apparatus in microglia in MBH.

(G and H) The average cisterna size (H), but not cisterna number (G), of the Golgi apparatus in microglia in MBH is significantly bigger in microglia-*Lpl*-KD mice than in Ctrl mice on an HCHF diet. The area indicated by the dark arrow is amplified at the right.

Data are presented as mean \pm SEM. ** $p < 0.01$, *** $p < 0.001$. Unpaired t test was performed in all experiments. Scale bars, 2 μ m in (A) and (B) (left) and (F) (left) and 200 nm in (A) and (B) (right) and (C) and (F) (right).

microglia-*Lpl*-KD mice in comparison with Ctrl mice (Figures S4A and S4B). On an HCHF diet, we found significantly more dysmorphic mitochondria in MBH microglia in microglia-*Lpl*-KD mice compared with Ctrl mice (40% in Ctrl versus 65% in *Lpl*-KD mice; Figures 4A, 4B, and 4D). Moreover, the total number of mitochondria in each microglia per section tended to decrease in microglia-*Lpl*-KD mice (Figure S4C). Neurons near the microglia exhibited a similar percentage of dysmorphic mitochondria in microglia-*Lpl*-KD mice and Ctrl mice on a chow diet (Figures S4D–S4F). While on an HCHF diet, we found more dysmorphic mitochondria as well as more autophagosomes in neurons close to microglia in the MBH of microglia-*Lpl*-KD mice compared with Ctrl mice (Figures 4A, 4B, and 4E; Figures S4G–S4J). Because, upon HCHF diet stimulation, most of the reactive microglia are found adjacent to POMC neurons, we assume that many of

the microglia-adjacent neurons that possess dysmorphic mitochondria are POMC neurons.

***Lpl* Deletion Induces Swelling of the Golgi Apparatus on an HCHF Diet**

Interestingly, we also observed a dysmorphology of another important cell organelle—the Golgi apparatus. On an HCHF diet, the Golgi apparatus in microglia from microglia-*Lpl*-KD mouse MBH had a significantly larger cisterna size without changes in cisterna number (Figures 4F–4H), indicating a swelling of the microglial Golgi apparatus. The Golgi apparatus processes secretory proteins and lipids and is involved in the endocytic pathway and lysosome formation. Dysfunction of the Golgi apparatus in microglia with *Lpl* deletion may also contribute to the impaired phagocytic capacity in these cells.

DISCUSSION

Hypothalamic microglia activation is associated with diet-induced obesity (Gao et al., 2014; Thaler et al., 2012). However, whether microglia activation has detrimental effects on hypothalamic neurons is unclear. Here we provide evidence that LPL-regulated intracellular microglia metabolism is important for maintaining microglial immune responses in a hypercaloric environment. LPL seems to be particularly important for supporting its phagocytic capacity, which is fundamental for the clearance of cell debris. LPL is thus a key player in microglial immunometabolism, ensuring the homeostatic brain microenvironment that is necessary for optimal functioning of the neurons in the hypothalamus and other brain regions.

In the CNS, lipid metabolism is quite insulated from the circulation. LPL has been described to translocate to the luminal surface to hydrolyze VLDL in the blood. However, the translocation enzyme glycosylphosphatidylinositol-anchored glycoprotein has been reported to be undetectable in the CNS (Davies et al., 2010). Thus, although LPL is highly abundant in microglia, it might not be translocated through the blood-brain barrier to take up lipoproteins directly from the circulation. In addition, our fasting-refed test on an HCHF diet did not detect any difference between microglia-*Lpl*-KD and Ctrl mice, which also supports that LPL in microglia does not participate directly in the sensing of peripheral lipids. Thus, the majority of the lipoproteins hydrolyzed by microglial LPL are probably produced in the CNS.

Phospholipids are essential components of phagosome formation and remodeling (Boulais et al., 2010). Here we found that, in *Lpl*-KD microglia, the phospholipid content is profoundly reduced, and, concomitantly, the phagocytic capacity is downregulated. Thus, intact LPL-regulated phospholipid homeostasis is required for sufficient microglial phagocytosis. In *Lpl*-KD microglia, glutamine utilization is upregulated. In macrophages, glutamine is important for sustaining inflammatory responses (Rogerio et al., 2010; Wallace and Keast, 1992). Although, in *Lpl*-KD microglia, glutamine utilization was increased, the phospho-NF- κ B response to TNF- α stimulation was downregulated, indicating that microglial immune reactivity might require the presence of both glutamine and lipids.

In neurodegenerative disease, reactive microglia associated with inflammatory agents are considered a major cause of nearby neuronal death (Heneka et al., 2014). During acute neuronal injury, such as that caused by alcohol toxicity, both microglial activation and neurodegeneration are present (Ahlers et al., 2015). In mice that lack neuro-apoptosis, microglial activation is largely abolished. Thus, microglial activation is probably not the cause for the neural injury, but necessary for the removal of dead neurons and tissue recovery. We speculate that a similar microglia-neuron interactive mechanism is operative in microglia-*Lpl*-KD mice. On a chow diet, dysmorphic mitochondria are found in *Lpl*-KD microglia but not in nearby neurons, and the POMC neuron number is intact. This indicates that dysfunctional microglia are not the cause of POMC neuron loss. On an HCHF diet, when metabolic stress is induced, the neural debris generated by POMC neurons exceeds the clearance capacity of *Lpl*-KD microglia because of deficient microglial phagocytic capacity. POMC neurons will retain more dysmorphic mitochondria and other cell debris, as

indicated by an increase in autophagosomes, which might also be in charge of mitochondrial autophagy (mitophagy) and other intracellular pathological processes (Klionsky et al., 2014; Mizushima, 2007). All of these changes might eventually drive POMC neurons to enter a dysfunctional stage.

Previously, we have shown a loss of POMC neurons in wild-type mice after 4 months of HCHF diet (Yi et al., 2017). Our current data suggest that such HCHF-diet-induced POMC neuronal loss is accelerated when the nearby microglia are less reactive because of lack of LPL. α -melanocyte-stimulating hormones (α -MSHs) produced by POMC neurons decrease food intake and increase energy expenditure by binding to melanocortin receptors in discrete downstream areas. Intriguingly, microglia-*Lpl*-KD mice only had reduced heat production, but not increased food intake, as expected from POMC neuronal loss. This raises the possibility that other brain regions inside or outside of the hypothalamus exert inhibitory effects on food intake. Indeed, in microglia-*Lpl*-KD mice, we also observed morphological changes in hippocampal and cortical microglia, both on a chow and/or HCHF diet, indicating that other neural circuits outside of the hypothalamus might be involved in dysregulation of the energy balance. Eventually, the concerted changes inside and outside of the hypothalamic neural circuits resulted in enhanced metabolic disorders in microglia-*Lpl*-KD mice when on an HCHF diet.

Furthermore, the morphological changes in hippocampal and cortical microglia also indicate that cognitive functions in microglia-*Lpl*-KD mice may have changed. This possibility is supported by a recent study in which upregulation of *Lpl* gene expression in a unique cortical microglia population has been identified at an advanced stage of Alzheimer's disease (Keren-Shaul et al., 2017).

At least one remaining question that needs to be answered is how the lipid metabolic disorder caused by the *Lpl* deletion eventually results in mitochondrial dysmorphology. Among the major mitochondrial morphology-regulating genes, we found an upregulation of dynamin-related protein 1 (Drp1) (Figure S4K). Drp1 is a key mediator of mitochondrial fission, and a previous study showed that inhibition of Drp1 blocks cell death (Frank et al., 2001). Whether mitochondrial dysfunction in microglia-*Lpl*-KD mice is linked to increased Drp1 activity will be an important subject for future studies. In the current study, we only investigated the immune response and phagocytic capacity of *Lpl*-KD microglia, taking into account the importance of LPL-gated fatty acid production. Another important question is whether other microglial functions were altered in *Lpl*-KD microglia and can be attributed to part of the observed phenotype. Finally, in the current study, we exclusively studied male mice. Regarding the recent finding that estrogen receptor alpha regulation of body weight interacts with LPL-dependent lipid processing in the hypothalamus (Wang et al., 2016), it needs to be studied whether female microglia-*Lpl*-KD mice will present different microglial innate immunity in obesity.

EXPERIMENTAL PROCEDURES

Animals

Microglia-specific postnatal *Lpl*-KD mice were generated by crossing *Lpl*^{fl/fl} mice with *Cx3cr1*^{CreERT2} mice (provided by Prof. Steffen Jung, Weizmann

Institute of Science), which harbor the tamoxifen-inducible Cre recombinase driven by the chemokine (C-X3-C motif) receptor 1 (*Cx3cr1*) promoter (Yona et al., 2013). At the age of 6 weeks, tamoxifen was given by intraperitoneal (i.p.) injection for 5 days at a dose of 100 μ g per injection to excise the loxP site of *Lpl*. *Lpl* flox-homozygous and Cre-positive mice (*Lpl^{fl/fl}-Cx3cr1^{CreERT2}*) are referred to as the KD model. Their littermates, which were Cre-positive but had an *Lpl* wild-type sequence, served as Ctrl (*Cx3cr1^{CreERT2}*). All studies were approved by and performed according to the guidelines of the Institutional Animal Care and Use Committee of the Helmholtz Center (Munich, Bavaria, Germany).

Ex Vivo Microglial *Lpl* KD

Primary cells were isolated from neonatal *Lpl^{fl/fl}-Cx3cr1^{CreER}* and *Cx3cr1^{CreER}* mouse brains. When the mixed glial culture reached 90% confluency, L929 cell line conditioned medium was added to the regular modified eagle medium (MEM) (30% v/v) for 2 days to support microglial proliferation. After shaking and seeding, microglia were treated with MEM + 10% fetal calf serum (FCS) + 1% antibiotics + 1 μ M 4-hydroxytamoxifen for 5 consecutive days. Cells were then ready for experiments.

Plate-Based Respirometry

Oxygen consumption rate was recorded by a Seahorse XF analyzer to determine the microglial cellular respiration status. Microglia fuel dependency was tested with a fuel flex test kit (Seahorse Bioscience).

Statistical Analysis

All results are expressed as mean \pm SEM. Statistical comparisons were performed using one-way, two-way, or repeated ANOVA with GraphPad Prism (GraphPad, San Diego, California, USA). Unpaired Student's t test was performed unless indicated otherwise.

SUPPLEMENTAL INFORMATION

Supplemental Information includes Supplemental Experimental Procedures and four figures and can be found with this article online at <http://dx.doi.org/10.1016/j.celrep.2017.09.008>.

AUTHOR CONTRIBUTIONS

Y.G. performed mouse breeding, metabolic phenotyping, primary culture, cell respirometry, PCR, and western blotting. A.V.-I. and N.v.d.W. performed electron microscopy and analyzed the data. M.J.K. performed immunohistochemical and immunofluorescent staining. T.O.E. performed the lipid analysis. C.L., C.G.-C., and J.Y. performed mouse breeding and/or HCHF diet feeding. R.Z.T. performed cell isolation and cell culture. F.M.V., R.H.H., A.J.V., R.H.E., A.K., and S.M.H. provided intellectual input and guidance. C.-X.Y. conceptualized the project, supervised the experiments, interpreted the findings, and drafted the manuscript.

ACKNOWLEDGMENTS

C.X.Y. is supported by an AMC fellowship (2014) and the Dutch Diabetes Fonds (2015.82.1826). We thank Matthias H. Tschöp for intellectual input and Daisy Picavet and Henk van Veen for technical support.

Received: November 13, 2016

Revised: June 28, 2017

Accepted: August 31, 2017

Published: September 26, 2017

REFERENCES

Ahlers, K.E., Karaçay, B., Fuller, L., Bonthius, D.J., and Dailey, M.E. (2015). Transient activation of microglia following acute alcohol exposure in developing mouse neocortex is primarily driven by BAX-dependent neurodegeneration. *Glia* 63, 1694–1713.

Babaev, V.R., Fazio, S., Gleaves, L.A., Carter, K.J., Semenkovich, C.F., and Linton, M.F. (1999). Macrophage lipoprotein lipase promotes foam cell formation and atherosclerosis in vivo. *J. Clin. Invest.* 103, 1697–1705.

Boulais, J., Trost, M., Landry, C.R., Dieckmann, R., Levy, E.D., Soldati, T., Michnick, S.W., Thibault, P., and Desjardins, M. (2010). Molecular characterization of the evolution of phagosomes. *Mol. Syst. Biol.* 6, 423.

Davies, B.S., Beigneux, A.P., Barnes, R.H., 2nd, Tu, Y., Gin, P., Weinstein, M.M., Nobumori, C., Nyrén, R., Goldberg, I., Olivecrona, G., et al. (2010). GPIIIBP1 is responsible for the entry of lipoprotein lipase into capillaries. *Cell Metab.* 12, 42–52.

Frank, S., Gaume, B., Bergmann-Leitner, E.S., Leitner, W.W., Robert, E.G., Catez, F., Smith, C.L., and Youle, R.J. (2001). The role of dynamin-related protein 1, a mediator of mitochondrial fission, in apoptosis. *Dev. Cell* 1, 515–525.

Gao, Y., Ottaway, N., Schriever, S.C., Legutko, B., García-Cáceres, C., de la Fuente, E., Mergen, C., Bour, S., Thaler, J.P., Seeley, R.J., et al. (2014). Hormones and diet, but not body weight, control hypothalamic microglial activity. *Glia* 62, 17–25.

García-Cáceres, C., Quarta, C., Varela, L., Gao, Y., Gruber, T., Legutko, B., Jastroch, M., Johansson, P., Ninkovic, J., Yi, C.X., et al. (2016). Astrocytic Insulin Signaling Couples Brain Glucose Uptake with Nutrient Availability. *Cell* 166, 867–880.

Goldmann, T., Wieghofer, P., Müller, P.F., Wolf, Y., Varol, D., Yona, S., Brendecke, S.M., Kierdorf, K., Staszewski, O., Datta, M., et al. (2013). A new type of microglia gene targeting shows TAK1 to be pivotal in CNS autoimmune inflammation. *Nat. Neurosci.* 16, 1618–1626.

Hao, S., Dey, A., Yu, X., and Stranahan, A.M. (2016). Dietary obesity reversibly induces synaptic stripping by microglia and impairs hippocampal plasticity. *Brain Behav. Immun.* 51, 230–239.

Heneka, M.T., Kummer, M.P., and Latz, E. (2014). Innate immune activation in neurodegenerative disease. *Nat. Rev. Immunol.* 14, 463–477.

Heneka, M.T., Carson, M.J., El Khoury, J., Landreth, G.E., Brosseron, F., Feinstein, D.L., Jacobs, A.H., Wyss-Coray, T., Vitorica, J., Ransohoff, R.M., et al. (2015). Neuroinflammation in Alzheimer's disease. *Lancet Neurol.* 14, 388–405.

Keren-Shaul, H., Spinrad, A., Weiner, A., Matcovitch-Natan, O., Dvir-Szternfeld, R., Ulland, T.K., David, E., Baruch, K., Lara-Astaiso, D., Toth, B., et al. (2017). A Unique Microglia Type Associated with Restricting Development of Alzheimer's Disease. *Cell* 169, 1276–1290.e17.

Kettenmann, H., Hanisch, U.K., Noda, M., and Verkhratsky, A. (2011). Physiology of microglia. *Physiol. Rev.* 91, 461–553.

Klionsky, D.J., Eskelinen, E.L., and Deretic, V. (2014). Autophagosomes, phagosomes, autolysosomes, phagolysosomes, autophagolysosomes... wait, I'm confused. *Autophagy* 10, 549–551.

Kuno, R., Wang, J., Kawanokuchi, J., Takeuchi, H., Mizuno, T., and Suzumura, A. (2005). Autocrine activation of microglia by tumor necrosis factor- α . *J. Neuroimmunol.* 162, 89–96.

Li, Y., Du, X.F., Liu, C.S., Wen, Z.L., and Du, J.L. (2012). Reciprocal regulation between resting microglial dynamics and neuronal activity in vivo. *Dev. Cell* 23, 1189–1202.

Mizushima, N. (2007). Autophagy: process and function. *Genes Dev.* 21, 2861–2873.

Nakahira, K., Haspel, J.A., Rathinam, V.A., Lee, S.J., Dolinay, T., Lam, H.C., Englert, J.A., Rabinovitch, M., Cernadas, M., Kim, H.P., et al. (2011). Autophagy proteins regulate innate immune responses by inhibiting the release of mitochondrial DNA mediated by the NALP3 inflammasome. *Nat. Immunol.* 12, 222–230.

Newsholme, P., Curi, R., Gordon, S., and Newsholme, E.A. (1986). Metabolism of glucose, glutamine, long-chain fatty acids and ketone bodies by murine macrophages. *Biochem. J.* 239, 121–125.

O'Neill, L.A., Kishton, R.J., and Rathmell, J. (2016). A guide to immunometabolism for immunologists. *Nat. Rev. Immunol.* 16, 553–565.

Oren, R., Famham, A.E., Saito, K., Milofsky, E., and Karnovsky, M.L. (1963). Metabolic patterns in three types of phagocytizing cells. *J. Cell Biol.* 17, 487–501.

- Prinz, M., and Priller, J. (2014). Microglia and brain macrophages in the molecular age: from origin to neuropsychiatric disease. *Nat. Rev. Neurosci.* *15*, 300–312.
- Rogero, M.M., Borelli, P., Fock, R.A., Borges, M.C., Vinolo, M.A., Curi, R., Nakajima, K., Crisma, A.R., Ramos, A.D., and Tirapegui, J. (2010). Effects of glutamine on the nuclear factor-kappaB signaling pathway of murine peritoneal macrophages. *Amino Acids* *39*, 435–441.
- Thaler, J.P., Yi, C.X., Schur, E.A., Guyenet, S.J., Hwang, B.H., Dietrich, M.O., Zhao, X., Sarruf, D.A., Izgur, V., Maravilla, K.R., et al. (2012). Obesity is associated with hypothalamic injury in rodents and humans. *J. Clin. Invest.* *122*, 153–162.
- Tschöp, M.H., Speakman, J.R., Arch, J.R., Auwerx, J., Brüning, J.C., Chan, L., Eckel, R.H., Farese, R.V., Jr., Galgani, J.E., Hambly, C., et al. (2011). A guide to analysis of mouse energy metabolism. *Nat. Methods* *9*, 57–63.
- Valdearcos, M., Robblee, M.M., Benjamin, D.I., Nomura, D.K., Xu, A.W., and Koliwad, S.K. (2014). Microglia dictate the impact of saturated fat consumption on hypothalamic inflammation and neuronal function. *Cell Rep.* *9*, 2124–2138.
- Wallace, C., and Keast, D. (1992). Glutamine and macrophage function. *Metabolism* *41*, 1016–1020.
- Wang, H., and Eckel, R.H. (2009). Lipoprotein lipase: from gene to obesity. *Am. J. Physiol. Endocrinol. Metab.* *297*, E271–E288.
- Wang, H., Wang, Y., Taussig, M.D., and Eckel, R.H. (2016). Sex differences in obesity development in pair-fed neuronal lipoprotein lipase deficient mice. *Mol. Metab.* *5*, 1025–1032.
- West, A.P., Shadel, G.S., and Ghosh, S. (2011). Mitochondria in innate immune responses. *Nat. Rev. Immunol.* *11*, 389–402.
- Yi, C.X., Walter, M., Gao, Y., Pitra, S., Legutko, B., Kälin, S., Layritz, C., García-Cáceres, C., Bielohuby, M., Bidlingmaier, M., et al. (2017). TNF α drives mitochondrial stress in POMC neurons in obesity. *Nat. Commun.* *8*, 15143.
- Yona, S., Kim, K.W., Wolf, Y., Mildner, A., Varol, D., Breker, M., Strauss-Ayali, D., Viukov, S., Guillems, M., Misharin, A., et al. (2013). Fate mapping reveals origins and dynamics of monocytes and tissue macrophages under homeostasis. *Immunity* *38*, 79–91.
- Zhang, Y., Chen, K., Sloan, S.A., Bennett, M.L., Scholze, A.R., O’Keeffe, S., Phatnani, H.P., Guarnieri, P., Caneda, C., Ruderisch, N., et al. (2014). An RNA-sequencing transcriptome and splicing database of glia, neurons, and vascular cells of the cerebral cortex. *J. Neurosci.* *34*, 11929–11947.
- Zhang, Y., Sloan, S.A., Clarke, L.E., Caneda, C., Plaza, C.A., Blumenthal, P.D., Vogel, H., Steinberg, G.K., Edwards, M.S., Li, G., et al. (2016). Purification and Characterization of Progenitor and Mature Human Astrocytes Reveals Transcriptional and Functional Differences with Mouse. *Neuron* *89*, 37–53.